# Efficient Spatio-Temporal Signal Recognition on Edge Devices Using PointLCA-Net

Sanaz Mahmoodi Takaghaj, Jack Sampson

arXiv:2411.14585v2 [cs.LG] 13 Apr 2025

***Abstract*—Recent advancements in machine learning, particularly through deep learning architectures like PointNet, have transformed the processing of three-dimensional (3D) point clouds, significantly improving 3D object classification and segmentation tasks. While 3D point clouds provide detailed spatial information, spatio-temporal signals introduce a dynamic element that accounts for changes over time. However, applying deep learning techniques to spatio-temporal signals and deploying them on edge devices presents challenges, including real-time processing, memory capacity, and power consumption. To address these issues, this paper presents a novel approach that combines PointNet's feature extraction with the in-memory computing capabilities and energy efficiency of neuromorphic systems for spatio-temporal signal recognition.**

**The proposed method consists of a two-stage process: in the first stage, PointNet extracts features from the spatio-temporal signals, which are then stored in non-volatile memristor crossbar arrays. In the second stage, these features are processed by a single-layer spiking neural encoder-decoder that employs the Locally Competitive Algorithm (LCA) for efficient encoding and classification. This work integrates the strengths of both PointNet and LCA, enhancing computational efficiency and energy performance on edge devices. PointLCA-Net achieves high recognition accuracy for spatio-temporal data with substantially lower energy burden during both inference and training than comparable approaches, thus advancing the deployment of advanced neural architectures in energy-constrained environments.**

***Index Terms*—PointNet, LCA, Encoder, Decoder, Spatio-temporal data**

## I. Introduction

In recent years, the advent of deep learning has significantly advanced the analysis of complex data structures, with architectures such as PointNet [1] revolutionizing the processing of three-dimensional (3D) point clouds. PointNet is a powerful tool for extracting invariant features from unordered point cloud data, using a symmetric aggregation mechanism to capture the intrinsic properties of 3D objects. This capability has led to substantial improvements in tasks such as 3D object classification and segmentation [1]–[3], where handling irregular and unordered input is crucial.

Despite these advancements, applying such techniques in edge devices —- where energy efficiency is crucial —- remains constrained by the limitations of conventional computing systems on real-time processing of complex data. These limitations include challenges related to data movement, memory capacity, and power consumption. Conventional processors, such as CPUs and GPUs/TPUs, are optimized for handling dense, synchronized data structures through the effective utilization of instruction and data pipelines. However, their efficiency significantly diminishes when managing sparse, asynchronous event streams [4]. This calls for a departure from traditional von Neumann computing systems.

Recently, neuromorphic computing – drawing inspiration from the human brain's capabilities and/or structures -— has emerged as a transformative approach in computing, offering energy-efficient and massively parallel processing elements [5]. A new wave of neuromorphic processors [6]–[12] has been developed to deliver low-latency and low-power consumption, making them well-suited for modeling Spiking Neural Networks (SNNs) and processing sparse data streams from event-based sensors. SNNs represent a compelling paradigm for modeling temporal dynamics, providing advantages in processing sequential data through discrete spike events that emulate biological neural activity. Unlike traditional neural networks, SNNs compute with asynchronous spikes that are temporally precise as opposed to continuous-valued activations that operate on a common clock cycle. SNNs have the potential to excel at representing and processing temporal sequences, making them particularly well-suited for tasks involving dynamic patterns and time-varying signals.

Neuromorphic chips support neurons that generate asynchronous binary outputs (spikes). They enable the efficient execution of vector-matrix multiplication (VMM) operations, also known as multiply-and-accumulate (MAC) operations, which are fundamental to deep learning algorithms, by leveraging a crossbar array of memory elements [13]. Non-volatile memory elements, such as PCM [14]–[16] and RRAM [17]–[20], have been proposed for integration into synapse and neuron circuits [21]. However, most efforts to apply in-memory computing to SNNs have focused on unsupervised learning using local learning rules, such as Spike-Timing Dependent Plasticity (STDP) [22] which adjusts a synaptic weight of a neuron based on the relative timing between its inputs and outputs. Nonetheless, STDP-based learning rules face limited scalability and applicability to complex learning tasks such as 3D object classification or recognizing spatio-temporal signals.

This paper presents a novel algorithm (PointLCA-Net) that leverages PointNet for feature extraction and integrates these features with in-memory computing and neuromorphic processing to address the challenges of recognizing spatio-temporal signals on these platforms. These features are extracted once and stored on non-volatile memory elements, allowing for in-memory computation on neuromorphic platforms that prioritize specialized operations and energy-efficient processing. We propose a two-stage approach where spatio-temporal data, such as that from DVS cameras, is initially preprocessed and converted into 3D point cloud data. In the first stage, PointNet generates

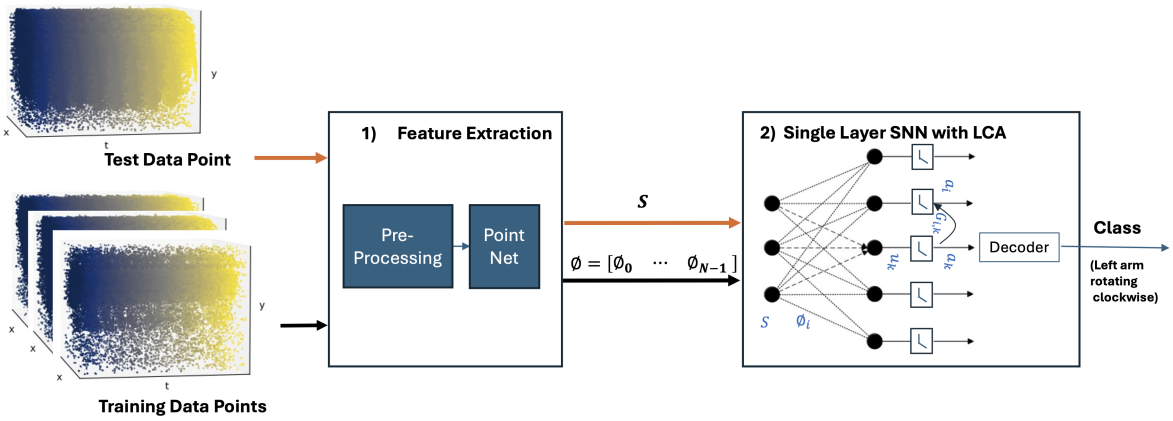


Fig. 1. PointLCA-Net Architecture: Features ($\phi_i$) are extracted once and stored in the synaptic weights of a single-layer SNN for inference. The orange arrows indicate the inference process that follows the completion of training (feature extraction).

robust feature representations from this 3D point cloud data. These features, which capture both geometric and semantic information, are then input into a single-layer SNN encoder-decoder architecture in the second stage for classification tasks.

Neuromorphic operation on sparse data should likewise exhibit and exploit sparsity. To that end, we consider approaches that employ the Locally Competitive Algorithm (LCA) [24] as the encoder to ensure that only a limited number of neurons are active at any given time, enabling sparsity and efficient coding of high-dimensional data. One proposal for working with these sparse LCA encodings is the Exemplar LCA-Decoder [23]. Used as a single-layer encoder-decoder, it is a computational model that iteratively updates neuron activity to find a sparse representation of the input data (i.e, encoding) and then uses these neuron activities for classification tasks (i.e, decoding).

The objective of this study is to evaluate PointLCA-Net and assess the efficacy of integrating PointNet's feature extraction with the efficiency of sparse coding through LCA in a manner that is deployable on edge devices. By feeding features derived from PointNet into a single-layer SNN model, we aim to achieve high recognition accuracy for spatio-temporal data while maintaining low computational overhead and energy efficiency. In summary, the contribution of this paper is a novel approach to PointNets that integrates the Winner-Take-All mechanism from SNNs. This contribution improves the computational efficiency of PointNets, making them more suitable for deployment on embedded systems.

## II. Related Work

Only a modest number of recent works have studied how to apply SNNs to point clouds, primarily due to the prohibitive computational overhead involved in training. Wang et al. [25] proposed a method for constructing Space-time Event Clouds (SECs) from event camera data and employed the original PointNet [1] and the hierarchical PointNet++ [2] architectures for gesture recognition tasks.

Spiking PointNet [26] is the first spiking neural network model designed for efficient deep learning on point clouds. The model is trained using a single time step, and membrane potential perturbation is introduced to enhance its performance. It offers significant speedup and storage savings during the training phase and, in certain experiments, surpasses its DNN counterpart, demonstrating the potential of SNNs for point cloud tasks. However, using single time-step training limits the model's ability to capture complex temporal dynamics. Additionally, the inherent complexity of training SNNs in this fashion may become prohibitive when applied to more complex datasets beyond the ModelNet10 and ModelNet40 datasets tested in that work.

SpikePoint [27] employs a SNN architecture specifically designed for event camera action recognition. The use of surrogate gradients in this approach involves computing the derivative of a surrogate function, which can be computationally expensive, particularly for complex architectures such as PointNet. Furthermore, the accuracy and convergence of training with surrogate gradients is sensitive to the choice of surrogate function's parameters, potentially leading to additional computational costs for tuning and optimization.

## III. PointLCA-Net

Fig. 1 shows the architecture of PointLCA-Net. The spatio-temporal training data is pre-processed and sent to PointNet for feature extraction. These features are then stored in the synaptic weights of a single-layer spiking neural network with LCA encoding and used for classifying (unseen) test inputs.

### A. Feature Extraction

Fig. 2 illustrates the feature extraction process using the PointNet [1] architecture, which processes 3D point cloud data by first aligning the data into a canonical space using an input transformation network (Input Transform). Each point is then independently processed through shared Multi-Layer Perceptrons (MLPs) and feature transformation network (Feature Transform) to extract point-wise features. These features are aggregated using a symmetric function (Max Pooling), to produce a permutation-invariant global feature vector. The resulting 1024-dimensional feature vector captures comprehensive geometric and semantic information of the point cloud.

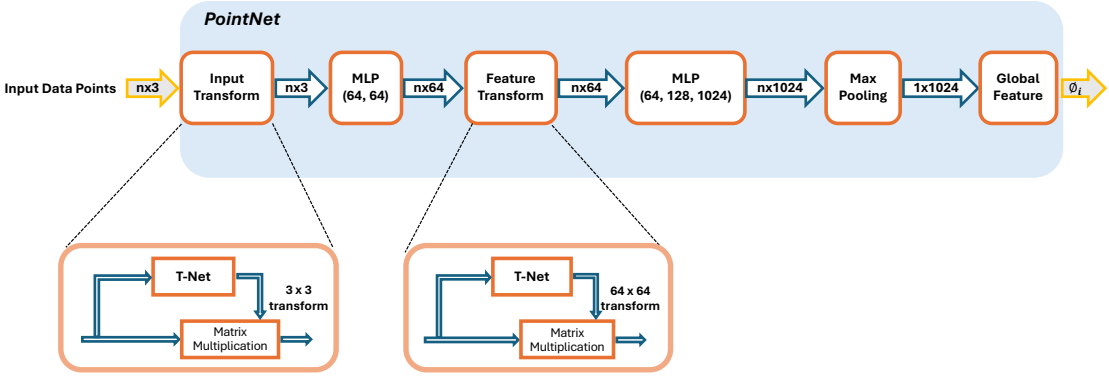


Fig. 2. Feature Extraction using PointNet.

These features $\phi_i$ are then used to construct the dictionary $\phi$ (Eq. 5).

### B. Single-Layer SNN with LCA Encoder and Decoder

We first provide an overview of the Exemplar LCA-Decoder algorithm [23], which utilizes the sparse coding algorithm [24] and the LCA algorithm [28] to represent the input signal $S$:

$$S = \sum_{i=0}^{M-1} \phi_i a_i + \varepsilon \tag{1}$$

where $\phi$ is a dictionary of features ($\phi_i$) and $a_i$ represents the activation of the LIF neuron $i$. The term $\varepsilon$ represents Gaussian noise. The LIF neuron's membrane potential $u_i$ is subject to a driving excitatory input $b_i$ and an inhibition matrix (Gramian) $G$. The Gramian matrix allows stronger neurons to prevent weaker neurons from becoming active, resulting in a sparse representation.

$$\tau \dot{u}_i[k] + u_i[k] = b_i - \sum_{m \neq i}^{M-1} G_{i,m} a_m[k] \tag{2}$$

$$b_i = S\phi_i \tag{3}$$

$$G = \phi^T \phi \tag{4}$$

$$\phi = [\phi_0, \phi_1, \ldots, \phi_{M-1}] \tag{5}$$

Each $\phi_i$ represents a feature learned from a data point in the training dataset. This approach eliminates the need for dictionary learning, differing from the original LCA, where Stochastic Gradient Descent (SGD) is used to learn and update the dictionary for each batch of input data. The thresholding function is:

$$\begin{aligned} a_i[k] &= T_\lambda(u_i[k]) \\ &= \begin{cases} u_i[k] - \lambda\,\mathrm{sign}(u_i[k]), & |u_i[k]| \geq \lambda \\ 0, & |u_i[k]| < \lambda \end{cases} \end{aligned} \tag{6}$$

Here, the threshold $\lambda$ refers to the level that the membrane potential must exceed for the neuron to become active. Next, a decoder is designed to decode the sparse codes $a_i$ and map them to $K$ distinct classes from the training dataset. Later, the same decoder is used to generate predictions or classifications for the unseen test data points.

Given a sufficient number of training data points $M$, each test data point will have a sparse coding representation $a = [a_0, a_1, a_2, ..., a_{M-1}]$, where the majority of the $a_i$ values will be zero. Ideally, for any test input $S_{Test}$, the non-zero entries in the vector $a$ would correspond exclusively to the dictionary atoms $\phi_i$ associated with class $k$, where $k$ ranges from 1 to $K$. However, modeling errors and input signal noise may introduce small non-zero entries that are associated with multiple classes. To address this issue and better harness the relevance of neuron activations for each class, the "Maximum Sum of Activations" decoder is proposed. In this approach, the $\ell_1$ norms of the activations for each class $k$ are summed and the class with the highest value is determined:

$$Predicted\ Class = \underset{k}{argmax}\Big(\sum_i \left|a_i^{(k)}\right|\Big) \tag{7}$$

## IV. Experiment Setup

We evaluated our work using PyTorch [29] and the following datasets: NMNIST [30], DVS128 [6] and Spiking Heidelberg Digits (SHD) [31]. Event streams in these spatio-temporal datasets are treated as space-time event clouds, where each event is represented by its spatial coordinates (x, y) and temporal component (t). We concatenate theses coordinates into a tensor of shape (x, y, t) for processing. Due to the temporal variability inherent in these datasets, we preprocess the data by standardizing the input size to ensure uniformity for training and evaluation.

### A. Dataset Pre-Processing

The preprocessing phase begins by evaluating the duration of the events. Based on this assessment, the data is segmented into smaller windows, with the sizes and numbers of these windows determined by the event duration. Each window is then sampled to select a fixed number of events (128, 256, 512, or 1024). These sampled events are concatenated, shuffled and downsampled to create a final subset of 1024 events, which is subsequently input into the PointNet for feature extraction.

TABLE I
TOP-1 TEST ACCURACY SCORES FOR POINTLCA-NET.

| | | | | Accuracy | |
|---|---|---|---|---|---|
| | | | | Decoding Methods | |
| **Dataset** | **Method** | **GFLOPs** | **Energy** | $\max_i \{a_i\}$ | $\max_k \sum_i \left\lvert a_i^{(k)} \right\rvert$ |
| NMNIST | PointLCA-Net | 3 | 0.27 mJ | 95.49% | **98.01%** |
| DVS128 | PointLCA-Net | 0.7 | 0.065 mJ | 82.67% | **90.02%** |
| SHD | PointLCA-Net | 0.07 | $6.4\,\mu$J | 59.85% | **65.11%** |
| DVS128 | SpikePoint [27][a] | 0.9 | 0.82 mJ | **98.6%** | |

[a]This method hasn't been tested on NMNIST or SHD.

TABLE II
HYPERPARAMETERS

| Symbols | Description | Value |
|---|---|---|
| $\lambda$ | Threshold | 0.2 |
| $\tau$ | Leakage | 1000 |
| $k$ | Number of time steps | 100 |

### B. NMNIST

The NMNIST dataset is a spiking variant of the MNIST dataset, generated by presenting images to a neuromorphic vision camera equipped with the ATIS (Asynchronous Time-based Image Sensor). This dataset comprises 60,000 training images, each consisting of 300 time samples, along with 10,000 test images used for accuracy evaluation.

### C. DVS128

The DVS128 dataset, captured using a Dynamic Vision Sensor (DVS) camera, includes recordings of 11 distinct hand gestures, with approximately 20,000 to 40,000 events per gesture class. It contains 1,176 samples allocated for training and 288 samples for testing.

### D. Spiking Heidelberg Digits (SHD)

The SHD dataset comprises spoken digits from zero to nine in both English and German. Audio waveforms within the dataset are transformed into spike trains using an artificial cochlea model. The dataset includes 8,156 training samples and 2,264 test samples, each with varying temporal duration.

## V. EVALUATION

Table I displays the energy estimation and accuracy performance across all datasets. All experiments were consistently conducted using the hyperparameters specified in Table II. These hyperparameters were selected to achieve near 100% training accuracy, with the results demonstrating the test accuracy. Further tuning of these hyperparameters could potentially enhance accuracy for each dataset even further. Additionally, Table I shows that the "Maximum Sum of Activations" decoder yields significantly improved results across all datasets compared to the "Maximum Activation" decoder. The energy estimation was calculated based on the computed floating point operations during inference (Table III) and the expected energy consumption per floating point operation, which is discussed in detail in the following section.

### A. Workload and Energy Efficiency Analysis

In this section, we conduct a comprehensive evaluation of the workload and energy efficiency of PointLCA-Net. We assess the workload efficiency by estimating the number of Floating-Point Operations (FLOPs) and follow this with a discussion of energy consumption.

Computing $b_i$ in Eq. 3 requires $N * M$ multiplications and $(N-1) * M$ addition, where $N$ is the global feature size and $M$ represents the length of the dictionary (also the number of spiking neurons). The inhibition signal calculation in Eq. 2 involves $M^2 - M$ multiplications and $M^2 - 2M$ additions. Additionally, the leakage term introduces $M$ multiplication operations, while $3M$ additions are required to combine these terms and update the neurons' membrane potentials, as specified in Eq. 2. Furthermore, computing the Gramian matrix $G$ in Eq.4 entails $\frac{M(M+1)N}{2}$ multiplications and $\frac{M(M+1)(N-1)}{2}$ additions.

$$\underset{(Training)}{FLOPs} = \frac{M(M+1)(2N-1)}{2} \tag{8}$$

This computation, considered part of the training cost and performed once per task (dataset), is excluded from the inference cost. Thus, the total floating-point operations required per time step $K$ for inference is given by:

$$\underset{(Inferenec)}{FLOPs} = K(\frac{(2N-1)M}{K} + 2M^2 + M) \tag{9}$$

Note that $b_i$ is computed once per input data and remains constant across iterations. Finally, the expected sparsity through LCA is factored in by redefining $M$, the number of active neurons, as $\hat{M}$, which represents the average number of firing neurons whose $a_m \neq 0$.

$$\underset{(Inferenec)}{FLOPs} = K(\frac{(2N-1)M}{K} + 2M\hat{M} + M) \tag{10}$$

Table III displays the estimated training and inference FLOPs for PointLCA-Net. "TFLOPs" denotes the Tera FLOPs required to compute the Gramian matrix, while "GFLOPs" represents the Giga FLOPs for inference operations. Training FLOPs accounts for all training data points, whereas inference FLOPs is estimated for a single test input. We conducted two scenarios with 100 and 10 time steps (*K*). Reducing the number of time steps from 100 to 10 resulted in an average reduction of 80% in inference GFLOPs. Additionally, the sparsity induced by LCA

TABLE III
WORKLOAD ANALYSIS OF POINTLCA-NET

| Dataset | Training (TFLOPs) | K | N | M | $\hat{M}$[a] | Inference (GFLOPs) |
|---|---|---|---|---|---|---|
| NMNIST | 3.7 | 100 | 1024 | 60K | 240 | 3 |
| | | 10 | 1024 | 60K | 240 | 0.4 |
| DVS128 | 0.84 | 100 | 1024 | 28.6K | 114 | 0.7 |
| | | 10 | 1024 | 28.6K | 114 | 0.12 |
| SHD | 0.07 | 100 | 1024 | 8.156K | 33 | 0.07 |
| | | 10 | 1024 | 8.156K | 33 | 0.02 |

[a] From [23], we assumed that 0.4% of neurons spike at each time step.

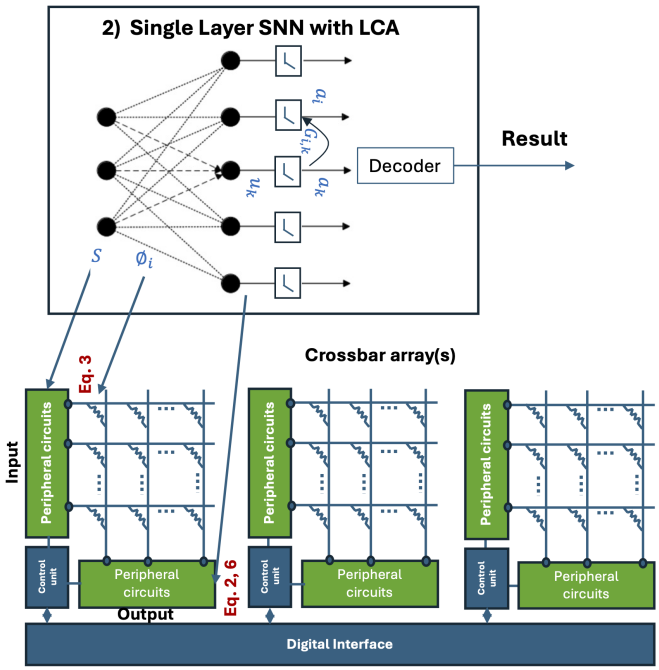


Fig. 3. PointLCA-Net Hardware Deployment

led to an average reduction of 99.54% in computational effort during inference.

In addition to the improvement in workload efficiency, PointLCA-Net leverages recent advancements in in-memory computing through memristive crossbar arrays. Memristive crossbars can perform multiplication operations based on Ohm's Law (I = V · G, where I is the current, V is the input voltage, and G is the conductance of each memristor), thereby enhancing energy efficiency and reducing the area footprint. Yao et al. [32] reported an energy efficiency of 11 Tera FLOPs per Watt for MAC operations using RRAM crossbar arrays. This is equivalent to each floating point operation consuming approximately $9.09 \times 10^{-14}$ joules of energy.

Fig. 3 illustrates the hardware mapping of PointLCA-Net, where the $\phi_i$ values are represented as the conductance of memristors in each column and are used for neuron excitatory input multiplications in Eq. 3. Inputs are preprocessed in the input peripheral circuits, while neuron dynamics and thresholding (as defined in Eq. 2 and Eq. 6) are implemented in the output peripheral circuits in the neural processor. The calculation of the Gramian matrix, which serves as the training head in this algorithm, can be performed offline, with the results stored in a lookup table (LUT) in the on-chip memory of the host processor.

## VI. DISCUSSION

We successfully evaluated PointLCA-Net on spatio-temporal data using the NMNIST, DVS128, and SHD datasets. While this work marks the first application of PointNet to NMNIST and SHD, SpikePoint [27], a variant of PointNets designed for SNNs, has been tested on the DVS128 dataset. SpikePoint utilizes a surrogate training method, achieving an accuracy of 98.6% with a GFLOPs value of 0.9, compared to 0.7 for PointLCA-Net. However, its estimated dynamic energy consumption is 0.82 mJ, approximately 12.62 times greater than that of PointLCA-Net. Additionally, Wang et al. [25] reported an accuracy of 90.20% on the DVS128 dataset with 10 classes using the original PointNet, and 97.08% with PointNet++ through a proposed rolling buffer framework. Although this work was the first to apply PointNet to spatio-temporal data, it did not address hardware deployment, leaving the energy efficiency of the approach unknown.

This study serves as a proof of concept and has significant potential as an algorithm that can be uniformly applied to various spatio-temporal data, including video and audio. However, it has limitations in accuracy compared to the state of the art, and further improvements could be achieved by exploring alternative architectures for feature extraction, such as PointNet++ [2] and Point Transformer [33]. PointNet++ is a hierarchical extension of PointNet that applies the architecture recursively to a nested partitioning of the input set and adaptively combines features from multiple scales. Unlike PointNet's single-stage processing that aggregates features globally with simpler operations, PointNet++ processes points in local neighborhoods, performing additional clustering and multi-scale feature extraction. This hierarchical approach increases the number of operations and memory usage, leading to a higher computational load. While we didn't explore using PointNet++ features in this work, it is an area of interest for future research.

Finally, in this study, we utilized the entire set of training data points to construct the dictionary. While larger dictionary lengths can improve accuracy, they may also create a computational burden for large datasets. To enhance computational efficiency, one potential approach is to reduce the dictionary length $M$ through Principal Component Analysis (PCA), Support Vector Machines (SVM), or by selecting discriminative features, thereby decreasing the computational overhead. For instance, a 10% reduction in dictionary length could, on average, reduce inference FLOPs by 17% and training FLOPs by 20%. As a result, this opens up new avenues for enhancing computational efficiency and model performance in future studies.

## VII. CONCLUSION

In this work, we explored integrating LCA with PointNets for the first time and assessed its performance on classification tasks using the NMNIST, DVS128, and SHD datasets. We utilized features extracted through PointNet within an LCA encoder-decoder framework, which eliminated the need for

training a dictionary as done in the original LCA. Additionally, we demonstrated how this approach can be mapped to memristor crossbar arrays for efficient in-memory computing on edge devices. This study highlights the potential for further research, including the investigation of alternative architectures such as PointNet++ and Point Transformer for higher accuracy. Given the energy efficiency potential of PointLCA-Net and its adaptability to various datasets, it presents an opportunity for enhancement in spatio-temporal data classification.

## REFERENCES


[1] C. R. Qi, H. Su, K. Mo, and L. J. Guibas, "PointNet: Deep learning on point sets for 3D classification and segmentation," in *Proceedings of the IEEE Conference on Computer Vision and Pattern Recognition*, pp. 652–660, 2017.

[2] C. R. Qi, L. Yi, H. Su, and L. J. Guibas, "PointNet++: Deep hierarchical feature learning on point sets in a metric space," *Advances in Neural Information Processing Systems*, vol. 30, 2017.

[3] X. Ma, C. Qin, H. You, H. Ran, and Y. Fu, "Rethinking network design and local geometry in point cloud: A simple residual MLP framework," *arXiv preprint arXiv:2202.07123*, 2022.

[4] S. Dave, R. Baghdadi, T. Nowatzki, S. Avancha, A. Shrivastava, and B. Li, "Hardware acceleration of sparse and irregular tensor computations of ML models: A survey and insights," *Proc. IEEE*, vol. 109, no. 10, pp. 1706–1752, 2021.

[5] Zheng, Nan and Mazumder, Pinaki. *Learning in energy-efficient neuromorphic computing: algorithm and architecture co-design*. John Wiley & Sons, 2019.

[6] A. Amir, B. Taba, D. Berg, T. Melano, J. McKinstry, C. Di Nolfo, T. Nayak, A. Andreopoulos, G. Garreau, M. Mendoza, and others, "A low power, fully event-based gesture recognition system," in *Proc. IEEE Conf. Comput. Vision Pattern Recognit.*, 2017, pp. 7243–7252.

[7] M. Davies, N. Srinivasa, T.-H. Lin, G. Chinya, Y. Cao, S. H. Choday, G. Dimou, P. Joshi, N. Imam, S. Jain, and others, "Loihi: A neuromorphic manycore processor with on-chip learning," *IEEE Micro*, vol. 38, no. 1, pp. 82–99, 2018.

[8] S. B. Furber, F. Galluppi, S. Temple, and L. A. Plana, "The SpiNNaker project," *Proc. IEEE*, vol. 102, no. 5, pp. 652–665, 2014.

[9] S. Höppner *et al.*, "The SpiNNaker 2 processing element architecture for hybrid digital neuromorphic computing," *arXiv preprint arXiv:2103.08392*, 2021.

[10] R. Khaddam-Aljameh, M. Stanisavljevic, J. F. Mas, G. Karunaratne, M. Brändli, F. Liu, A. Singh, S. M. Müller, U. Egger, A. Petropoulos, and others, "HERMES-core—A 1.59-TOPS/mm² PCM on 14-nm CMOS in-memory compute core using 300-ps/LSB linearized CCO-based ADCs," *IEEE J. Solid-State Circuits*, vol. 57, no. 4, pp. 1027–1038, 2022.

[11] M. Le Gallo, R. Khaddam-Aljameh, M. Stanisavljevic, A. Vasilopoulos, B. Kersting, M. Dazzi, G. Karunaratne, M. Brändli, A. Singh, S. M. Mueller, and others, "A 64-core mixed-signal in-memory compute chip based on phase-change memory for deep neural network inference," *Nature Electronics*, vol. 6, no. 9, pp. 680–693, 2023.

[12] J. Pei, L. Deng, S. Song, M. Zhao, Y. Zhang, S. Wu, G. Wang, Z. Zou, Z. Wu, W. He, and others, "Towards artificial general intelligence with hybrid Tianjic chip architecture," *Nature*, vol. 572, no. 7767, pp. 106–111, 2019.

[13] Aguirre, Fernando, Sebastian, Abu, Le Gallo, Manuel, Song, Wenhao, Wang, Tong, Yang, J. Joshua, Lu, Wei, Chang, Meng-Fan, Ielmini, Daniele, Yang, Yuchao, et al. *Hardware implementation of memristor-based artificial neural networks*. *Nature Communications*, vol. 15, no. 1, p. 1974, 2024.

[14] S. Kim *et al.*, "NVM neuromorphic core with 64k-cell (256-by-256) phase change memory synaptic array with on-chip neuron circuits for continuous in-situ learning," in *Proc. Int. Electron Devices Meeting (IEDM)*, 2015, pp. 17–1.

[15] D. Kuzum, R. G. Jeyasingh, B. Lee, and H.-S. P. Wong, "Nanoelectronic programmable synapses based on phase change materials for brain-inspired computing," *Nano Lett.*, vol. 12, no. 5, pp. 2179–2186, May 2011.

[16] T. Tuma, M. Le Gallo, A. Sebastian, and E. Eleftheriou, "Detecting correlations using phase-change neurons and synapses," *IEEE Electron Device Lett.*, vol. 37, no. 10, pp. 1238–1241, Oct. 2016.

[17] E. Covi *et al.*, "Analog memristive synapse in spiking networks implementing unsupervised learning," *Front. Neurosci.*, vol. 10, p. 482, 2016.

[18] A. Pantazi, S. Woźniak, T. Tuma, and E. Eleftheriou, "All-memristive neuromorphic computing with level-tuned neurons," *Nanotechnology*, vol. 27, no. 35, p. 355205, 2016, IOP Publishing.

[19] M. Rao, H. Tang, J. Wu, W. Song, M. Zhang, W. Yin, Y. Zhuo, F. Kiani, B. Chen, X. Jiang, and others, "Thousands of conductance levels in memristors integrated on CMOS," *Nature*, vol. 615, no. 7954, pp. 823–829, 2023.

[20] A. Serb *et al.*, "Unsupervised learning in probabilistic neural networks with multi-state metal-oxide memristive synapses," *Nature Communications*, vol. 7, p. 12611, 2016.

[21] Sebastian, Abu, Le Gallo, Manuel, Khaddam-Aljameh, Riduan, and Eleftheriou, Evangelos. "Memory devices and applications for in-memory computing." *Nature Nanotechnology* 15, no. 7 (2020): 529–544. Nature Publishing Group UK London.

[22] Indiveri, Giacomo, and Liu, Shih-Chii. "Memory and information processing in neuromorphic systems." *Proceedings of the IEEE* 103, no. 8 (2015): 1379–1397. IEEE.

[23] S. M. Takaghaj and J. Sampson, "Exemplar LCA-Decoder: A Scalable Framework for On-Chip Learning," *arXiv preprint arXiv:2406.10066*, 2024.

[24] C. J. Rozell, D. H. Johnson, R. G. Baraniuk, and B. A. Olshausen, "Sparse coding via thresholding and local competition in neural circuits," *Neural Computation*, vol. 20, no. 10, pp. 2526–2563, 2008.

[25] Q. Wang, Y. Zhang, J. Yuan, and Y. Lu, "Space-time event clouds for gesture recognition: From RGB cameras to event cameras," in *2019 IEEE Winter Conference on Applications of Computer Vision (WACV)*, 2019, pp. 1826–1835.

[26] D. Ren, Z. Ma, Y. Chen, W. Peng, X. Liu, Y. Zhang, and Y. Guo, "Spiking pointnet: Spiking neural networks for point clouds," *Advances in Neural Information Processing Systems*, vol. 36, 2024.

[27] H. Ren, Y. Zhou, X. Lin, Y. Huang, H. Fu, J. Song, and B. Cheng, "SpikePoint: An Efficient Point-based Spiking Neural Network for Event Cameras Action Recognition," in *Proc. of the Twelfth International Conference on Learning Representations*, 2024.

[28] C. Rozell, D. Johnson, R. Baraniuk, and B. Olshausen, "Locally Competitive Algorithms for Sparse Approximation," in *Proc. 2007 IEEE Int. Conf. Image Processing*, vol. 4, pp. IV-169–IV-172, 2007, doi: 10.1109/ICIP.2007.4379981.

[29] A. Paszke, S. Gross, F. Massa, A. Lerer, J. Bradbury, G. Chanan, T. Killeen, Z. Lin, N. Gimelshein, L. Antiga, and others, "PyTorch: An imperative style, high-performance deep learning library," *Advances in Neural Information Processing Systems*, vol. 32, 2019.

[30] G. Orchard, A. Jayawant, G. K. Cohen, and N. Thakor, "Converting Static Image Datasets to Spiking Neuromorphic Datasets Using Saccades," *Frontiers in Neuroscience*, vol. 9, p. 437, 2015."

[31] B. Cramer, Y. Stradmann, J. Schemmel, and F. Zenke, "The Heidelberg Spiking Data Sets for the Systematic Evaluation of Spiking Neural Networks," *IEEE Transactions on Neural Networks and Learning Systems*, vol. 33, no. 7, pp. 2744–2757, 2020.

[32] Yao, Peng, Wu, Huaqiang, Gao, Bin, Tang, Jianshi, Zhang, Qingtian, Zhang, Wenqiang, Yang, J. Joshua, and Qian, He. *Fully hardware-implemented memristor convolutional neural network*. *Nature*, vol. 577, no. 7792, pp. 641–646, 2020. Nature Publishing Group UK London.

[33] H. Zhao, L. Jiang, J. Jia, P. H. S. Torr, and V. Koltun, "Point Transformer," in *Proceedings of the IEEE/CVF International Conference on Computer Vision*, pp. 16259–16268, 2021.